

# MULTIVARIABLE AUTOPILOT DESIGN AND IMPLEMENTATION FOR TACTICAL MISSILES

Friedrich S. Kramer\*  
Raytheon Systems Company  
Tewksbury, Massachusetts 01876

## Abstract

A tactical skid-to-turn missile autopilot is designed and implemented using a two step design process that results in an optimal output feedback with a fixed, low-order dynamic compensator for reduced design and implementation cost. The gain design consists of minimizing a performance index in which measurements and controls are appropriately weighted to achieve the desired speed of response, while minimizing overshoot, fin rates, body rates, and maximizing stability margins. The cross channel multivariable autopilot provides faster response times with better stability than does the single channel classical autopilot. The faster response time results in many performance benefits, including smaller miss distance that results in increased lethality, and reduced homing time requirements. This autopilot was implemented and tested in missile-borne microprocessors.

## Introduction

The multivariable autopilot design and implementation for a tactical tail controlled missile described in this paper is the result of several years of internal development during the late eighties and early nineties. This work represents the genesis for all multivariable design developments at Raytheon that include Patriot Anti-Cruise Missile, Standard Missile Block IV and IV-A, and Enhanced Fiber Optic Guided Missile Programs. The outcome of this extensive development effort is a common software architecture that is general across all missiles. This common architecture is based on the classical Raytheon 3-loop autopilot that is implemented in most tactical missiles and provides a basis for leveraging existing designs. The actual implementations vary depending upon the missile programs legacy and the background of the designers but all are founded on common principles.

Copyright © 1998 by the Raytheon Company. Published by the American Institute of Aeronautics and Astronautics, Inc. with permission.

\* Manager, Guidance, Navigation and Control Department.  
Senior Member AIAA

Although based on a linear quadratic optimization, newer techniques such as Mu, and H-infinity, are readily being adapted to this autopilot topology.

## Performance Improvements

A fast responding missile is a key component in intercepting low observable, high velocity, maneuvering targets. The late acquisition of low observable targets and those employing countermeasures reduces terminal acquisition range and hence available homing time. High terminal closing velocity further reduces the homing time available. A key performance measure requires that 8 to 10 guidance time constants are available for a lethal miss distance provided that the missile has sufficient lateral acceleration (approximately 2 to 3 times the target maneuver depending on the quality of the onboard sensors and guidance algorithms) available. An integral part in reducing the guidance time constant is reducing the missile acceleration response time.

This cross-coupled multivariable autopilot topology for a surface-to-air missile achieves substantial response improvements over a classical autopilot topology for the same missile, actuators, and instruments. Only complete software change to the autopilot is necessary. The non-minimum phase characteristics of tail control missiles limit the lateral acceleration response, which is referred to as the "wrong way effect". A further improvement in missile acceleration response time requires a structural change in the missile such as adding divert-thrusters forward of its center-of-gravity.

The lateral acceleration performance advantages of the cross-coupled multivariable design are illustrated in Figure 1, for a 10 gee step command. The nonlinear 6 degree-of-freedom simulation results for this 12 km altitude and cross-coupled -22.5 degree wind angle orientation shows that the 63% and 95%

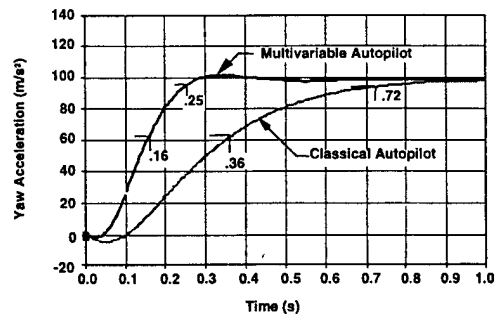


Fig. 1 Achieved more than twice the acceleration response improvement with multivariable autopilot.

rise times for the multivariable design have been improved over the current system by factors of 2.5 and 3, respectively.

The homing missile analyzed in this paper has cruciform tail control surfaces and employs a skid-to-turn steering policy using three orthogonal axes -- roll, yaw, and pitch. Roll rate regulators maintains a specified rate, usually zero, and commanded by guidance. The yaw and pitch axis controllers track acceleration commands generated by the guidance law.

In order to provide a form, fit and function replacement, the multivariable autopilot is designed using the same open loop crossover frequencies as the current, classically designed, autopilot. The open loop frequency response for the loop broken at the roll, yaw, and pitch fin angle commands is shown in Figure 2. The maximum singular values of the returned difference for the roll, yaw and pitch channels are plotted at each frequency. For tail controlled missiles, these plots have interpretations similar to Bode diagrams. Experience has shown that breaking the loop on at a time and applying classical gain and phase margin analysis is an acceptable indicator of stability when used in conjunction with root-summed square tolerance techniques. Both the multivariable design and the current system singular values cross over and roll off at similar frequencies. The low frequency pitch and yaw singular values of the multivariable design are 10 to 15 dB higher than the current system indicating better lateral acceleration performance.

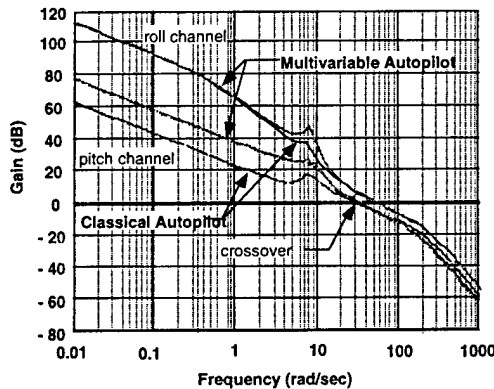


Fig. 2 Low frequency gain improvement with same crossover frequencies.

### Multivariable Autopilot Architecture

The multivariable autopilot is a roll, yaw, and pitch cross-coupled multi-loop matrix generalization of the

standard Raytheon three-loop scalar autopilot. This approach allows the gains to be optimally designed by applying the concepts and techniques from multivariable control theory while incorporating the design experience learned from the Raytheon three-loop autopilot. Since the multivariable design reduces to the current architecture when cross-coupling paths are set to zero, a direct comparison between the two designs can be made. Figure 3 shows how the autopilot is interconnected with the onboard instruments of the missile. The primary loops are the acceleration loop (outermost), synthetic stability loop (middle), and rate loop (innermost). There are three separate control channels: roll, yaw, and pitch. The roll channel regulates the roll rate, and maintains it at zero.

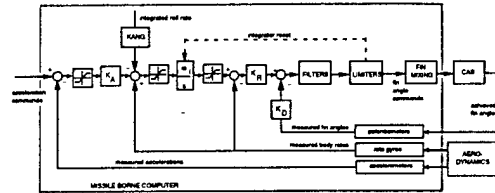


Fig. 3 Multivariable autopilot is a matrix implementation of the 3-loop autopilot.

In Figure 3, the autopilot gains blocks represent matrices. For example, the rate loop gain,  $K_R$ , is a 3 x 3 matrix and is expanded as shown below:

$$K_R = \begin{bmatrix} K_{R_{rr}} & K_{R_{ry}} & K_{R_{rp}} \\ K_{R_{yr}} & K_{R_{yy}} & K_{R_{yp}} \\ K_{R_{pr}} & K_{R_{py}} & K_{R_{pp}} \end{bmatrix}$$

In the above notation, the direct gain  $K_{R_{rr}}$  is the roll rate into roll fin command and the cross-coupled gain  $K_{R_{rp}}$  is the pitch rate into roll fin command. The direct gains are similar to the current gains in a classically designed three-loop autopilot. The cross-coupled gains are new to the three-loop autopilot design and contribute to the increased performance and improved stability. The cross-coupling gains are a product of the nonlinear optimization of the fully coupled linearized airframe model and are a function of angle-of-attack and aerodynamic wind angle. The direct roll gain  $K_{R_{rr}}$  is a essentially function of angle-of-attack only (Figure 4). However, the direct pitch and yaw gains (e.g.  $K_{R_{yy}}$ ) and all the cross-coupled gains (e.g.  $K_{R_{rp}}$ ) are functions of both angle-of-attack and wind angle. The 90-degree symmetry associated with each gain is exploited to reduce storage requirements in the missile

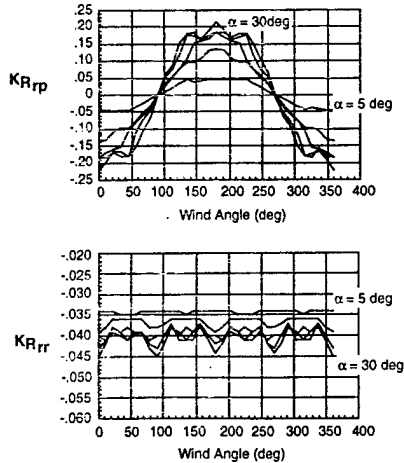


Fig. 4 Cross-coupled gains are strong functions of angle-of-attack and wind angle.

borne computer. The other gain matrices such as  $K_A$ ,  $W_I$ , and  $K_D$  follow similar patterns.

### Design Process and Analysis

#### Design Methodology Overview

The autopilot gain synthesis method consists of a two-step procedure. The first step calculates the feedback gain matrix based on a full state feedback topology. Full state feedback algorithms are computationally quick and don't suffer from requiring an initial stabilizing gain associated with output feedback methods. The second step uses known output feedback methods<sup>1,2</sup> and performs an approximate loop transfer recovery<sup>3</sup> of the stability margins that are characteristic of full-state feedback designs while providing a compensator with an order that is lower than the Linear-Quadratic-Gaussian/Loop-Transfer-Recovery method<sup>4</sup>. This allows transformation of the feedback gains to an architecture that becomes, when certain gains are set to zero, the current Raytheon three-loop autopilot. These features provide an optimal and robust design while reducing the complexity of the compensator, making the implementation practical.

#### 1<sup>st</sup> Step: Full state feedback design

In the first step, a full state feedback design produces a fast responding, robust system. (Figure 5). In this step, we apply any method that provides

satisfying results such as Linear Quadratic or H-infinity<sup>5</sup> optimization. Here, the full state feedback control law,

$$\delta_c = F^* x$$

given by the matrix  $F^*$ , is calculated by minimizing the Linear Quadratic performance index:

$$J = \int_0^{\infty} [x^T Q x + \delta_c^T R \delta_c] dt$$

The "full state" matrix assumes perfect knowledge of all terms. The weighting matrices  $Q$  and  $R$  are adjusted in the quadratic cost function to obtain the desired loop crossover frequencies and performance. A linear set of coupled first order equations denote the missile dynamics:

$$\begin{aligned} \dot{x} &= Ax + B\delta_c & x &\in \mathfrak{R}^n, \delta_c \in \mathfrak{R}^3 \\ y &= Cx & y &\in \mathfrak{R}^3 \end{aligned}$$

The state vector,  $x$ , represents the integrals of yaw and pitch accelerations, integrals of roll, yaw and pitch body rates, roll, yaw and pitch body rates, fin angles, fin rates and any other parasitic or frequency shaping terms. The output vector,  $y$ , represents the measured inertial instrument values of yaw and pitch accelerations, and roll, yaw and pitch body rates, as well as the potentiometer measured fin angles. The control  $\delta_c$  represents the roll, yaw and pitch fin commands.

A key part of this first step is the modeling of the state equations so that the compensator architecture has a structure that includes the Raytheon three-loop autopilot as a special case. A linear perturbation model of the airframe is derived from derived from wind tunnel test data. The linear state equations that are used consist of a fifth-order airframe model that includes aerodynamic, kinematic, and inertial coupling between the roll, yaw, and pitch degrees of freedom. These equations are then augmented with a second order actuator model. Placing integrators before each actuator augments the state equations. This integral

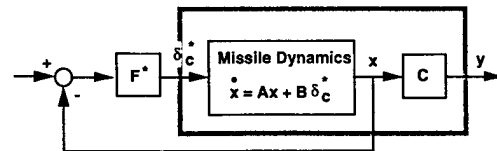


Fig. 5 Step 1 - full state feedback design.

compensation provides an automatic trim to deal with nonzero set points. A similarity transformation is then applied to the state equations to convert the aerodynamic angle-of-attacks, body rates, and fin angles to integrals of acceleration, integrals of body rates and body rates.

### 2<sup>nd</sup> Step: Output feedback with loop recovery

The second step is the design of a compensator filter that uses only the available measurements,  $y$ , to give the fastest response possible within the design constraints such as overshoot, fin rates and body rates. This consists of using linear-quadratic optimization, but with output feedback, to match the full-state feedback response that was designed in the first step (Figure 6). This step is a loop recovery technique using a third order compensator to achieve high performance and reduced control activity with minimum size and complexity. A Linear Quadratic performance index is set up to minimize the error between the full state feedback and compensator designs, i.e.

$$J = E \left\{ \int_0^{\infty} [e^T e + \rho u_c^T u_c] dt \right\}$$

The error,  $e$ , between the desired full state feedback control law  $\delta_c^*$  and the compensator control law  $\delta_c$  is minimized with the scalar parameter  $\rho > 0$  controlling the compensator bandwidth. This cost functional minimizes the mean-square-error between the control input and its full-state optimal value, and the mean-square filter input. Note that there is only a single free parameter in this cost, the loop recovery factor  $\rho$ , which provides a trade off between the penalties on the two errors.

Reduced order compensator<sup>6</sup> is designed using only the available measurements,  $y$ :

$$\begin{aligned} u &= -I_3 z & u &\in \mathcal{R}^3 \\ \dot{z} &= u & z &\in \mathcal{R}^3 \\ u_c &= -Ny - P_z z & u_c &\in \mathcal{R}^3 \end{aligned}$$

The missile and compensator states are

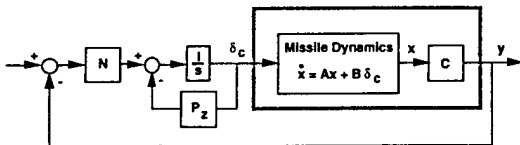


Fig. 6 Step 2 - Output feedback with loop recovery of reduced order compensator.

combined to form an augmented system

$$\begin{aligned} \dot{\tilde{x}} &= \tilde{A}\tilde{x} + \tilde{B}u_c & \tilde{x} &\in \mathcal{R}^{n+3} \\ \tilde{y} &= \tilde{C}\tilde{x} & \tilde{y} &\in \mathcal{R}^{8+3} \end{aligned}$$

where

$$\tilde{A} = \begin{bmatrix} A & B \\ 0 & 0 \end{bmatrix} \quad \tilde{B} = \begin{bmatrix} 0 \\ I_3 \end{bmatrix} \quad \tilde{C} = \begin{bmatrix} C & 0 \\ 0 & I_3 \end{bmatrix}$$

This optimization problem can be solved to get an output feedback control law having the form:

$$u_c = \tilde{G}\tilde{y} \quad u_c \in \mathcal{R}^3$$

The matrix gains  $N$  and  $P_z$  are embedded in the optimal output feedback gain matrix matrix:

$$\tilde{G} = [N \quad P_z]$$

We formulate an extension of the Raytheon three-loop autopilot by partitioning  $N$ :

$$N = [N_A \quad N_R \quad N_I \quad N_D]$$

where  $N_A$  is 3x2 and  $N_R, N_I, N_D$  are each 3x3. The matrix  $N$  is partitioned and converted to  $K_A, W_I, K_R$  and  $K_D$  matrices using similarity transformations.

$$K_A = N_I^{-1} N_A \quad (3x2)$$

$$K_R = P_z^{-1} N_R \quad (3x3)$$

$$W_I = N_R^{-1} N_I \quad (3x3)$$

$$K_D = P_z^{-1} N_D \quad (3x3)$$

### Linear Quadratic Performance Index Selection

The two-step design methodology above uses optimal output feedback, through a judicious choice of compensators placed before the actuator inputs, to recover the stability margin properties offered by the full-state linear-quadratic design. This formulation by itself does not incorporate the requirements imposed by constraints on the state variables; however, this formulation does provide free parameters in the cost functionals in the form of weighting matrices. As a result, these parameters can be utilized to maximize the autopilot performance subject to the state constraints.

The free parameters consist of the  $Q$  and  $R$  weighting matrices in the cost functional for the initial state feedback design, and the  $\rho$  parameter in the output

feedback cost functional. Since there are 196 elements in the Q matrix and nine elements to the R matrix, this gives us a total of 205 free parameters. The problem becomes one of reducing the complexity introduced by the large number of free parameters. Trade studies show that almost all of these parameters either have a negligible impact on autopilot performance or introduce unwanted couplings between the roll, yaw, and pitch degrees of freedom. By setting these parameters to zero, and by using the same weights for pitch and yaw, the Q and R matrices take on the following form:

$$Q = \text{diag}[Q_{11} \quad Q_{33} \quad Q_{33} \quad 1 \quad 1 \quad 0_9]$$

$$R = \text{diag}[R_{11} \quad R_{22} \quad R_{33}]$$

The number of free parameters are reduced to six: the integral yaw or pitch acceleration weight  $Q_{11}$ , the integral roll rate weight  $Q_{33}$ , the elements along the diagonal of the R-matrix corresponding to the pitch, yaw and roll commands, and  $\rho$ . The fourth and fifth parameters in Q are normalized to unity.

The parameter with the strongest effect is the loop recovery factor  $\rho$  because it affects the greatest number of autopilot characteristics. These include lateral acceleration response time, autopilot crossover frequencies, acceleration overshoots, missile body rates, and control actuator fin rates. A strategy for optimizing the set of free parameters is to start with varying the other weights at fixed values of  $\rho$ . This gives optimal values of the other weights and autopilot characteristics as a function of  $\rho$ . The optimal value of the loop recovery factor are then estimated based on these results.

Next in order of the strength of their effect are the Q-matrix elements  $Q_{11}$  and  $Q_{33}$ . Since the fourth element of the Q matrix is normalized to unity, the parameter  $Q_{33}$  becomes the ratio of the penalty on the

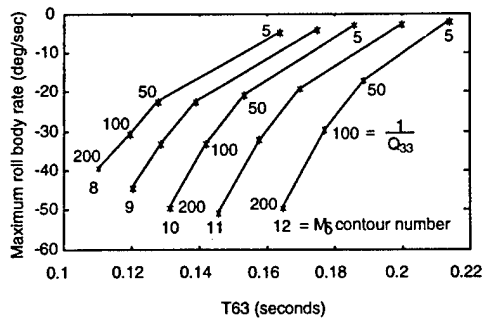


Fig. 7 Decreasing the maximum roll body rate increases the 63% rise time.

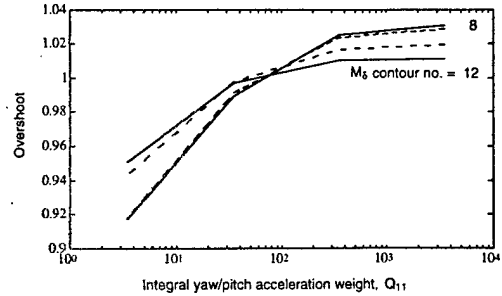


Fig. 8 Select  $Q_{11}$  to eliminate overshoot

integral of the roll rate to the penalty on the integral of the lateral body rate. Increasing the parameter  $Q_{33}$  reduces the maximum roll rate due to yaw and pitch inputs and also influences the crossover frequencies. This maximum roll rate reduction comes at the expense of the response times in yaw and pitch (Figure 7).

The parameter  $Q_{11}$  is the ratio of the penalty on the integral of yaw acceleration over the penalty on the integral of the yaw body rate. The effect of increasing  $Q_{11}$  is to increase the overshoot, decrease response time, increase yaw and pitch fin rates. The effect of  $Q_{11}$  on the overshoot is shown in Figure 8.

The weight  $Q_{11}$  does not buy much improvement in maximum yaw body rate by trading it off against rise time as is illustrated in Figure 9. As one would expect, increasing performance (reducing the t63 % rise time) reduces the stability margins (Figure 10).

The parameters that have the weakest effect are the R-matrix elements in that each element affects primarily only one crossover frequency. That is, the roll loop crossover frequency is a strong function of the weight on the roll fin deflection, the yaw loop crossover is a strong function of the yaw fin weight, and the pitch loop crossover is a strong function of the pitch fin weight.

These properties are convenient in that they

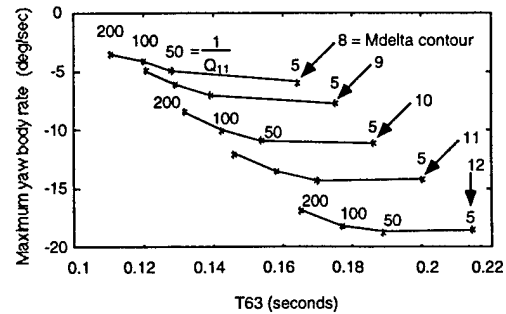


Fig. 9 Maximum yaw body rate tradeoff with response time.

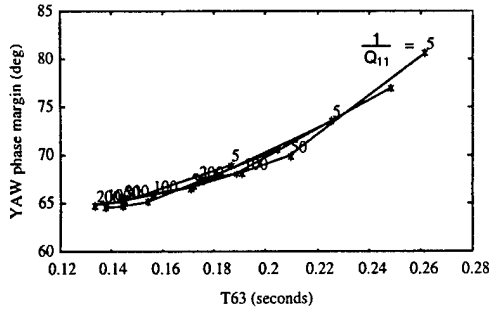


Fig. 10 Yaw phase margin decrease with reduced response time.

allow us to numerically adjust the control weighting matrix R matrix to obtain the desired crossover frequencies while choosing  $Q_{11}$  and  $Q_{33}$  to minimize overshoot, fin rates, and body rates. It is important to hold the crossovers constant because of the desire to prevent the crossovers from increasing to values that can cause instabilities due to structural modes or uncertainties in high-frequency dynamics due to fin servos, gyros, and accelerometers.

Optimization Methodology

The way the parameters Q, R, and  $\rho$  affect the autopilot performance and constrained states allows the design optimization problem to be decomposed into smaller, simpler optimization problems. These problems are simpler in that they involve only one or two free parameters. This motivates the types of algorithms to be used to optimize the weights. The strategy used to determine the optimal weights is determined next. First the loop recovery factor  $\rho$  that has the strongest effect is chosen and the optimization of the other weights is performed at this value. Second, a sequence of one-dimensional minimization is performed. Adjustments in  $Q_{11}$  and  $Q_{33}$  and the R matrix elements are alternated in order to minimize roll body rate and to drive the crossovers, overshoot, yaw fin rate, and pitch fin rate to within the tolerances given above. A one-dimensional minimization in  $Q_{11}$  is performed to determine the best compromise between overshoot and fin rate. This is followed by optimization of the R matrix elements in order to hold the crossovers to within 1 radian per second of the design requirement. The  $Q_{11}$  minimization with crossover correction is then repeated. Next, a one-dimensional minimization of roll body rate is performed using  $Q_{33}$ . This is again followed by a crossover correction using the R-matrix. This entire process is then repeated until the design

requirements are met. This gives an approximate solution, which can be further refined, if necessary, by using a multidimensional search scheme, such as the Levenburg-Marquardt algorithm. This method simultaneously optimizes the five free parameters in the Q and R matrices for a constant value of  $\rho$ .

Performance Results

A comparison of the performance of the multivariable autopilot versus the classical three-loop autopilot is summarized in Table 1. The multivariable design offers superior or comparable performance in virtually all measures. A key to the multivariable autopilot design is the performance improvement is not at the expense of increased open loop crossover frequencies. All the performance improvement comes from coupling the roll, yaw and pitch channels to improve the low (aerodynamic) frequency gain. This result is representative of the multivariable designs that have been obtained.

Table 1 Multivariable autopilot performance improvement for same classical crossovers

Parameter	Multi-variable	Classical
63% rise time (s)	0.15	0.36
95% rise time (s)	0.22	0.72
Max yaw fin rate (deg/s)	32	13
Roll crossover (rad/s)	46	46
Yaw crossover (rad/s)	26	26
Roll phase margin (deg)	58	37
Yaw phase margin (deg)	67	68
Roll gain margin (dB)	19	16
Yaw gain margin (dB)	24	21
15 deg angle of attack		
-22.5 wind angle		

The multivariable autopilot gains were calculated over the intercept flight envelope. Step responses were generated for one-half maximum achievable lateral acceleration commands and are graphed as a function of dynamic pressure (Figure 11). The multivariable autopilot is approximately twice as fast as the classical single channel design for the same open loop crossover frequencies as depicted in Table 1. The variation in the classical autopilot is a result of band switching the gains. The higher interpolation rate of the multivariable configuration provides a more

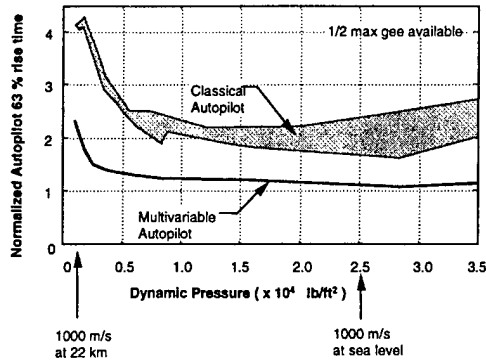


Fig. 11 The multivariable autopilot provides consistent fast response over intercept envelope. The nonlinear implementation is discussed in the next section.

### Nonlinear Implementation

#### Limiters

The implementation of a linearly optimized autopilot requires the use of limiters to prevent loop saturation that invalidates the design and cause the missile to lose control. Actuator fin angle and rate limiting, integrator anti-windup, and acceleration command limiting are all key.

Fin limiters are incorporated into the design to ensure that each of the missile's four fins do not exceed maximum angle and rate limits. The roll channel fin command is limited to a maximum fin deflection and angular rate. Then, this limited roll command is used to determine the proper fin rate and angle limits for the pitch and yaw channels. This method ensures that no channel will exceed the fin deflection limit. This method also preserves the direction of the commanded acceleration vector since the pitch and yaw channels are reduced by the same percentage when limiting is performed. This ensures that the missile will continue to follow the guidance command direction although the limiting process will slow the response.

Limiters were introduced into the autopilot design before and after the integrators in the synthetic stability path. These limiters maintain system stability in the presence of the large guidance step commands that may be received on the digital uplink of the SAM system. The limiters keep the missile rotational rates at or below the maximum gyroscopic limits. In this way the missile does not lose angular position or rate reference. The post stability-path-integrator limiter effects are also included in the anti-windup logic that is used when fin limiting occurs. This ensures that the

anti-windup logic does not cause the integrator output limits to be exceeded.

The directionality of the lateral acceleration commands is maintained by the use of proportional limiting in the synthetic stability paths similar to that used in the acceleration loop. The larger of the commanded values is determined and, if necessary, reduced to the predetermined maximum (limit) value. The other channel is then proportionally reduced. The same logic is used on the output of the synthetic stability.

An acceleration command limiter was added to the autopilot design to limit the rate of change of the acceleration commands. The command rate limiter compares the acceleration command of each channel (pitch and yaw) with its respective value from the previous minor cycle. If the magnitude of the difference is larger than the limit, the magnitude of the acceleration command passed through to the autopilot is recalculated to ensure that its rate of change is bounded. The other channel is then proportionally reduced to maintain the directionality of the original commands. If the rate of change is within the bounds, the limiter will not affect the command.

#### Angle-of-Attack and Wind Angle Estimates

Both missile total angle-of-attack and wind angle are needed onboard the missile to determine the correct set of autopilot gains. This information is not available on the uplink and there are no onboard instruments to determine it.

The relationship between trim level gees and missile total angle-of-attack is a function of the dynamic pressure. A least squares fit is made to the power series expansion (solving for the angle-of-attack) and two coefficients are stored for each of these zones then a parabolic fit can be made to the data. Using this method, estimates of the missile total angle-of-attack can be made with sufficient accuracy for use in the autopilot gain scheduling routines. In addition, because the relationships between trim level gees and total angle-of-attack is relatively invariant as a function of the wind angle  $\phi$ , only one curve is needed for each dynamic pressure band.

Wind angle estimates are calculated from acceleration measurements and are based on the ratio of lateral accelerations.

#### Implementation in a Missile Borne Computer

The multivariable autopilot is structured as a stored gain autopilot as opposed to an algorithmic autopilot. This type of autopilot architecture provides generality across missiles. The autopilot gains are a

function of altitude, velocity, angle-of-attack, and wind angle. Altitude and velocity are used to interpolate data tables so that gains can be determined based on the aerodynamic estimates of angle-of-attack and wind angle. These calculations are separated into critical and non-critical paths to insure the stability of the rate loops.

The multivariable autopilot was implemented entirely in software residing in two fixed-point 68020 microprocessors. The first processor uses uplinked data to interpolate gain tables for a specific Mach and altitude flight condition. This processor also uses inertial instrument data to estimate angle-of-attack and wind angle orientation for use in the gain interpolation. The gain-scheduling module in the first processor is separated into two processing rates – the uplink rate and the four minor cycle rate. During the uplink cycle, altitude and velocity are uplinked and an estimate of  $M_5$  is calculated on board the missile during this cycle. The interpolation of the gain tables by  $M_5$  reduces the storage requirements. This ensures that the crossover frequency remains fairly constant along an  $M_5$  contour since the rate loop gain time  $M_5$  approximates open loop crossover. Three dimensional constant gain tables are interpolated as functions of  $M_5$  to form intermediate two dimensional gain tables. These two dimensional intermediate tables are functions of angle-of-attack and wind angle. Gain interpolation uses the 90 degrees in wind angle, angle-of-attack and wind angle are used to interpolate the intermediate gain tables. The resulting

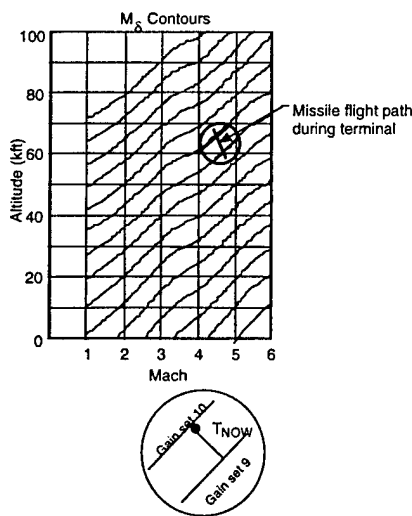


Fig. 12 Gains are interpolated over  $M_5$  contours.

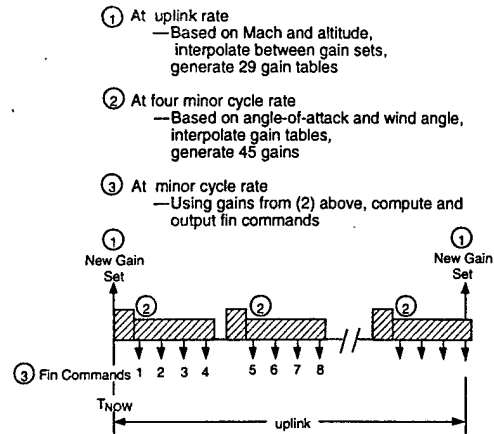


Fig. 13 Gains are interpolated at different time scales.

gains are sent to the second processor.

The second processor uses the instrument measurements and the autopilot algorithm to calculate the fin commands. The resulting gains are used in the critical and non-critical path calculations of the autopilot at a minor cycle rate to calculate fin commands. These calculations are separated into critical and non-critical paths to insure the stability of the high bandwidth loops. The calculations are done in fixed-point arithmetic. Computer critical path time is specified to minimize rate loop delays that can cause autopilot instabilities and the multivariable autopilot is well within this requirement. Figures 12 and 13 illustrate gain interpolation process.

Software specifications have been written for the multivariable autopilot. The code was evaluated in the MSFR/MRTS tests. An additional software specification was written in floating point for use by the 8800 processor. The unit and function tests of the individual program modules were tested at the digital subsystem level. Dynamic tests were performed that check, in fixed-point arithmetic, the notch depth and frequency of all the structural filters implemented. These dynamic tests showed that the notches are at the proper depth and frequency to attenuate structural feedback from missile vibrations in flight.

### Hardware / Software Missile Testing

#### Missile Stability and Frequency Response Tests

Missile Stability and Frequency Response (MSFR) tests were conducted on a full-up missile. These tests are needed to verify the autopilot closed loop stability in conjunction with the flexible bending

and torsion modes of the missile body. A flexible body model analytically determined the stability margins due to the body bending modes of the missile.

The missile was tested in a burnout configuration and was suspended above the ground using bungee cords. The Digital Subsystem used was a form-factored unit. All onboard instruments were present. A key result from the MSFR was the observation that the lateral channel oscillations coupled into the roll channel. Moving the structural filters into the feedback path eliminates this high frequency cross-feed.

#### Missile Round Test Set

At the Missile Round Test Set (MRTS) facility, a full-up guidance section was exercised through a series of automatic test scenarios under the control of the test equipment. The digital subsystem contained all of the normal operational software as well as the multivariable autopilot specific code. The missile was sequenced through a simulated launch and into the proper operational mode. During the time when the tests were conducted, the operational software, including uplink/downlink, major and minor cycle timing and telemetry was running.

A total of twelve tests were defined for evaluation of the multivariable autopilot in the MRTS facility. These 12 tests are divided into two distinct groups. The first eight dealt with the lateral channels of the autopilot while the last four dealt with the roll channel. The autopilot inputs for these tests could either be rates and accelerations emulated by software via serial I/O or generated using an actual Inertial Sensor Assembly (ISA) on a rate table.

The results of these tests compared well with predictions made by an autopilot simulation. In general the results from the test showed good agreement between the expected and the actual results. Those cases that showed poor agreement are attributed to differences resulting from the fixed-point arithmetic, biases in the instruments not modeled in the prediction simulation, and the truncated nature of the ISA instrument readings.

#### Simulation Performance Results

A high fidelity 6 degree-of-freedom simulation was used to simulate the multivariable autopilot performance improvements and compare the results against the current classical uncoupled autopilot. Both air-breathing targets (ABT) and tactical ballistic missile (TBM) intercepts were examined. Against the late acquisition of high altitude maneuvering TBM intercepts, the two-to-one improvements in lateral

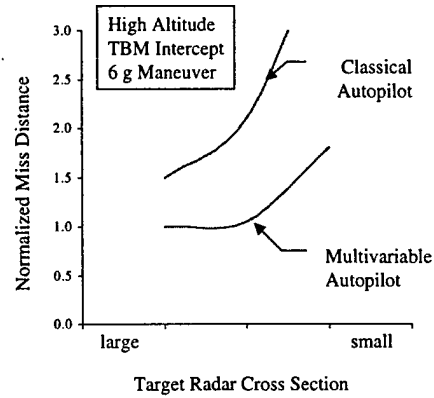


Fig. 14 The multivariable autopilot improves late acquisition performance.

acceleration response results in extending the performance capabilities (Figure 14). A time history comparison between the multivariable and classical autopilot against the same high altitude maneuvering TBM shows the improved acceleration command tracking. (Figure 15).

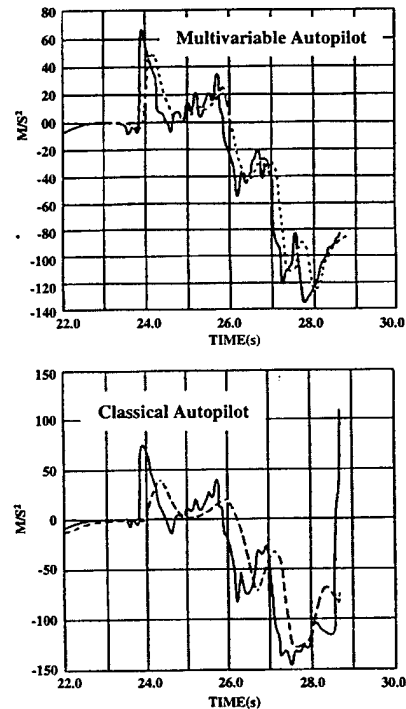


Fig. 15 The multivariable autopilot tracks acceleration commands to achieve small miss distances.

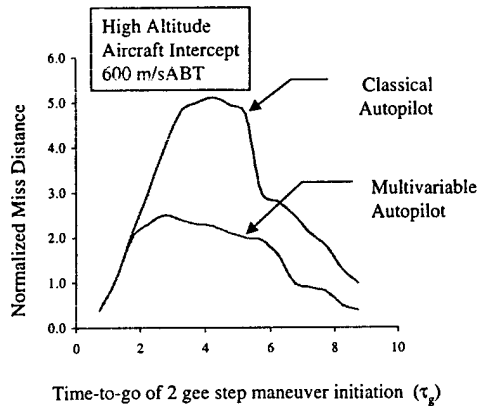


Fig. 16 The multivariable autopilot provides more than a 2:1 improvement in miss distance against evasive maneuvering ABTs.

Against high altitude ABT intercepts, a better than 2:1 improvement in miss distance is achievable with a faster responding airframe (Figure 16).

### Summary

The multivariable autopilot represents the current state of the art for missile autopilot design. It is the first multivariable design to be extensively evaluated and tested. This design is the result of extensive tradeoff studies that were used to generate the best performance obtainable within the physical constraints imposed by the existing hardware. The final architecture is a uniquely cross-coupled design.

The multivariable autopilot is designed to maintain constant performance over a range of altitude and Mach numbers using gains that are constant along fin effectiveness contours and that vary with angle-of-attack and wind angle. Response time is improved by a factor of two to three while maintaining current tactical missile roll bandwidth constraints, as well as all other dynamic limits, including body and fin rates. Gains are designed to explicitly use pitch-yaw-roll cross-coupling effects in the missile. Stability and performance tradeoff curves have been generated that aid in choosing MVAP gains.

### References

- <sup>1</sup> Levine, W.S., T.L. Johnson and M. Athans, "Optimal Limited State Variable Feedback Controllers for Linear Systems", *IEEE Trans. Automatic Control*, Vol. AC-16, December 1971.
- <sup>2</sup> Moerder, D.D., and A.J. Calise, "Convergence of a Numerical Algorithm for Calculating Optimal Output feedback Gains," *IEEE Trans. on Automatic Control*, Vol. AC-30, Sept. 1985.
- <sup>3</sup> Calise, A.J. and J.V.R. Prasad, "An Approximate Loop Transfer Recovery Method for Designing Fixed Order Compensators," *Journal of Guidance, Control and Dynamics*, Vol. 13, No. 2, Mar.-Apr. 1990.
- <sup>4</sup> Stein, G. and Athans, M., "The LQG/LTR Procedure for Multivariable Feedback Control Design," American Control Conference, San Diego, CA, June 1984.
- <sup>5</sup> Byrns Jr., E.V. and A.J. Calise, "Approximate Recovery of  $H_\infty$  Loop Shapes Using Fixed-Order Dynamic Compensation," *Journal of Guidance, Control and Dynamics*, Vol. 17, No. 3, May-Jun. 1994.
- <sup>6</sup> Kramer, F.S. and A.J. Calise, "Fixed Order Dynamic Compensation for Multivariable Linear Systems," *Journal of Guidance, Control and Dynamics*, Vol. 11, No. 1, Jan.-Feb. 1988.

AIAA 1998 Missile Sciences Conference

Title of Document MULTIVARIABLE AUTOPILOT DESIGN AND IMPLEMENTATION FOR TACTICAL MISSILES

PLEASE CHECK THE APPROPRIATE BLOCK BELOW:

- 1 copies are being forwarded. Indicate whether Statement A, B, C, D, E, F, or X applies.
- DISTRIBUTION STATEMENT A:  
APPROVED FOR PUBLIC RELEASE: DISTRIBUTION IS UNLIMITED
- DISTRIBUTION STATEMENT B:  
DISTRIBUTION AUTHORIZED TO U.S. GOVERNMENT AGENCIES ONLY; (Indicate Reason and Date). OTHER REQUESTS FOR THIS DOCUMENT SHALL BE REFERRED TO (Indicate Controlling DoD Office).
- DISTRIBUTION STATEMENT C:  
DISTRIBUTION AUTHORIZED TO U.S. GOVERNMENT AGENCIES AND THEIR CONTRACTORS; (Indicate Reason and Date). OTHER REQUESTS FOR THIS DOCUMENT SHALL BE REFERRED TO (Indicate Controlling DoD Office).
- DISTRIBUTION STATEMENT D:  
DISTRIBUTION AUTHORIZED TO DoD AND U.S. DoD CONTRACTORS ONLY; (Indicate Reason and Date). OTHER REQUESTS SHALL BE REFERRED TO (Indicate Controlling DoD Office).
- DISTRIBUTION STATEMENT E:  
DISTRIBUTION AUTHORIZED TO DoD COMPONENTS ONLY; (Indicate Reason and Date). OTHER REQUESTS SHALL BE REFERRED TO (Indicate Controlling DoD Office).
- DISTRIBUTION STATEMENT F:  
FURTHER DISSEMINATION ONLY AS DIRECTED BY (Indicate Controlling DoD Office and Date) or HIGHER DoD AUTHORITY.
- DISTRIBUTION STATEMENT X:  
DISTRIBUTION AUTHORIZED TO U.S. GOVERNMENT AGENCIES AND PRIVATE INDIVIDUALS OR ENTERPRISES ELIGIBLE TO OBTAIN EXPORT-CONTROLLED TECHNICAL DATA IN ACCORDANCE WITH DoD DIRECTIVE 5230.25, WITHHOLDING OF UNCLASSIFIED TECHNICAL DATA FROM PUBLIC DISCLOSURE, 6 Nov 1984 (Indicate date of determination). CONTROLLING DoD OFFICE IS (Indicate Controlling DoD Office).
- This document was previously forwarded to DTIC on \_\_\_\_\_ (date) and the AD number is \_\_\_\_\_.
- In accordance with provisions of DoD instructions, the document requested is not supplied because:
- It will be published at a later date. (Enter approximate date, if known).
- Other. (Give Reason)

DoD Directive 5230.24, "Distribution Statements on Technical Documents," 18 Mar 87, contains seven distribution statements, as described briefly above. Technical Documents must be assigned distribution statements.

 22 Sept 98.  
Authorized Signature/Date

FRIEDRICH S. KRAMER  
Print or Type Name  
978-858-4951  
Telephone Number

19981127 033



# Copyright Clearance and Release

MULTIVARIABLE AUTO PILOT DESIGN AND IMPLEMENTATION FOR TACTICAL MISSILES.

Paper No. AIAA-98-

Meeting AIAA 1998 MISSILE SCIENCES CONFERENCE

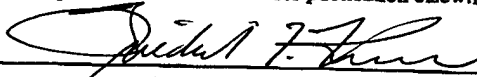
Return to: AIAA Technical Papers Specialist  
1801 Alexander Bell Drive, Suite 500  
Reston, VA 20191-4344

You must sign each of the following  
For your paper to be published:  
One copyright release form only (A, B, C, or D)

Clearance  
No-infringement statement

### CLEARANCE

This paper is UNCLASSIFIED (for public release) and has been cleared by the appropriate agencies, company, or government. It has not been published or submitted for publication elsewhere.

  
Signature of Author

21. Sept 98  
Date

### NO-INFRINGEMENT STATEMENT

Copyright laws recently have received fresh emphasis here and abroad. Please make unambiguous the copyright status of this work by signing the following affidavit assuring us that it contains no copyright-infringing material:

This paper represents original work by the author(s). No portion of the material is covered by a prior copyright; or for any portion copyrighted, the author has obtained permission for its use.

  
Signature of Author

21. Sept 98  
Date

### COPYRIGHT RELEASE

(Before signing, please read both sides of this form)

The copyright law effective January 1, 1978 gives the copyright of a paper or article to the person who wrote it. AIAA would like to continue its past policy of holding the copyright of any paper it publishes with the clear understanding that the author and his or her organization have the right to reproduce it for their own purposes, provided the reproductions are not for sale. Copyright Release Form A does this.

*N/A*

Copyright Release Form A: I assign copyright to my paper to AIAA, giving the Institute all rights to it except that I and the organization by which I was employed at the time I wrote the manuscript have the right of further reproductions, in part or in full, provided they are not for sale.

[Note: If Release Form A is signed, the copyright notice will read as follows: "Copyright © 19\_\_\_\_ by the American Institute of Aeronautics and Astronautics, Inc. All rights reserved."]

\_\_\_\_\_  
Signature of Author or Other Copyright Proprietor

\_\_\_\_\_  
Date

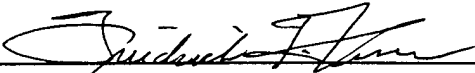
American Institute of Aeronautics and Astronautics  
1801 Alexander Bell Drive, Reston, VA 20191-4344  
Phone: 703/264-7500

(over)

Occasionally, special situations arise in which the author (or the author's organization, if the author has assigned his copyright to it) wishes to retain the copyright in his/her (or the organization's) name. In such a case, AIAA requires a license to publish the work. Copyright Release Form B should be used for this purpose.

✓ Copyright Release Form B: I hereby license AIAA to publish this paper and to use it for all of AIAA's current and future publication uses.

[Note: If the author or his company retains copyright (Release Form B), the copyright notice, in the name of the author, should appear at the bottom of the first page of the manuscript and should read as follows: "Copyright © 19\_\_\_\_ by \_\_\_\_\_. Published by the American Institute of Aeronautics and Astronautics, Inc., with permission."]

  
Signature of Author or Other Copyright Proprietor

21. Sept 98  
Date

### TO AUTHORS EMPLOYED BY GOVERNMENT AGENCIES

1. A "work of the United States Government" (hereinafter called a Government work) is a work prepared by an officer or employee of the United States Government as part of that person's official duties.
2. Copyright protection under the U.S. Copyright Law is not available for any Government work; however, copyright protection is available for a work of a Government employee that is done apart from his or her official duties, and the copyright shall reside in the employee (subject to any transfer made by the employee).
3. When a work of a Government employee does not fall within the purview of his or her official duties, the employee's use of Governmental time, material, or facilities will not, of itself, make the work a Government work.
4. Under the current copyright law a work may be protected, within certain limitations, even if a copyright notice is not present; however, the presence of a copyright notice on a work makes it clear to a reader who the copyright proprietor is and who can grant a license to reproduce the work, etc.
5. If a work of a Government employee is not a Government work, the AIAA will not publish the work unless the AIAA receives an assignment (Copyright Form A) or a license (Copyright Form B).
6. Copyright Form C is the appropriate form to be executed by a Government-employee author (except NASA employees) who has prepared a Government work.
7. Because of a master copyright agreement executed between NASA and AIAA, Copyright Form D is the appropriate form for NASA-employed authors submitting Government works.
8. Please execute one of the four forms. If you are uncertain as to whether the work was outside your official duties, the AIAA encourages you to seek appropriate counsel within your agency.

U/A

**Copyright Form C:** This paper is a work of the U.S. Government and is not subject to copyright protection in the United States. [Note: If Copyright Form C is signed, the notice will read as follows: "This paper is declared a work of the U.S. Government and is not subject to copyright protection in the United States."]

\_\_\_\_\_  
Signature of Author

\_\_\_\_\_  
Date

U/A

**Copyright Form D:** I am employed by NASA and prepared this work as part of my official duties. [Note: If Copyright Form D is signed, pursuant to the agreement between NASA and AIAA, the notice will read as follows: "Copyright © 19\_\_\_\_ by the American Institute of Aeronautics and Astronautics, Inc. No copyright is asserted in the United States under Title 17, U.S. Code. The U.S. Government has a royalty-free license to exercise all rights under the copyright claimed herein for Governmental purposes. All other rights are reserved by the copyright owner."]

\_\_\_\_\_  
Signature of Author

\_\_\_\_\_  
Date

4476